Current Research in Microbial Sciences 11 (2026) 100643

Contents lists available at ScienceDirect

Current Research in Microbial Sciences

journal homepage: www.sciencedirect.com/journal/current-research-in-microbial-sciences

Sublethal oxytetracycline and copper exposure alters rRNA gene copy number, expression, and intragenomic polymorphism in ciliates

Songbao Zou [a], Rao Fu [d], Huiwen Deng [b,c], Julin Yuan [a], Jun Gong [b,c,*]

[a] Agriculture Ministry Key Laboratory of Healthy Freshwater Aquaculture, Zhejiang Institute of Freshwater Fisheries, Huzhou, China
[b] School of Marine Sciences, Sun Yat-Sen University Zhuhai Campus, Tangjiawan, Zhuhai, 519082, China
[c] Southern Marine Science and Engineering Guangdong Laboratory (Zhuhai), Zhuhai, China
[d] Shandong Institute of Sericulture, Shandong Academy of Agricultural Sciences, Yantai, China

ARTICLE INFO

Keywords:
Protist
Ribosome RNA gene
Copy number
Intragenomic polymorphism
Metabarcoding biases

ABSTRACT

Ribosomal RNA (rRNA) genes serve as foundational markers for microbial eukaryotic diversity assessment, yet their responses to environmental stressors remain underexplored. This study examined the effects of sublethal oxytetracycline and $CuCl_2$ on phenotypic and ribotypic traits in the ciliated protists *Paramecium bursaria* and *Euplotes vannus* using single-cell quantitative PCR and high-throughput sequencing of 18S rDNA/rRNA. We found that both pollutants inhibited growth, enlarged cell volume, and elevated per-cell rDNA and rRNA copy numbers, but oxytetracycline selectively elevated rRNA: rDNA ratios. These effects increased the variance around established allometric scaling relationships between rDNA copy number and cell volume, without significantly altering the scaling slope. Intragenomic polymorphisms also increased, with the amplicon sequence variant (ASV) number of rRNA transcripts exceeding that of rDNA, and these elevated polymorphisms persisted post-stress relief. Re-analysis of field 18S metabarcoding data from $CuCl_2$-polluted marine biofilms revealed dose-dependent increases in the number of ASVs per operational taxonomic unit (OTU, defined at a cutoff of 97% sequence identity) in many protistan groups, suggesting that copper-induced mutagenic pressure on ribosomal RNA genes may prevail across diverse protistan taxa. Our findings imply that: (1) when interpreting ASV-based microbial diversity patterns, the potential for ASV richness inflation and elevated per-cell rDNA and rRNA abundances should be recognized as a likely consequence of exposure to environmental pollutants; (2) there is a potential for using the ASV-to-OTU number ratio in assessing environmental stress; and (3) metabarcoding of rRNA likely introduces more artificial ASVs than targeting rDNA. A combination of double metabarcoding of both rDNA and rRNA to identify active microbial members is recommended.

Introduction

Ribosomal RNA (rRNA) genes (or rDNA) are of evolutionary significance and have been the most popular molecular biomarkers for investigating the diversity and ecology of microbes in environmental samples (Pawlowski et al., 2012; Weider et al., 2005). These genes are present in hundreds to hundreds of thousands of copies in a eukaryotic genome (Gong et al., 2013) and are usually expressed to produce thousands to millions of rRNA transcripts in a vegetative cell (Zou et al., 2021). The rRNAs bind to many ribosomal proteins to form ribosomes, the molecular machines that are key to protein synthesis and cell proliferation. Recent single-cell analyses of ciliated protists (unicellular eukaryotes) have shown that several ribotypic traits (e.g., rDNA and rRNA copy number per cell, ratio of rRNA to rDNA copy numbers, and cellular rDNA or rRNA copy number per unit volume) are temperature- and life-cycle stage-dependent, but generally form scaling relationships with cellular or physiological traits, such as cell volume and growth rate (Fu and Gong, 2017; Zou et al., 2021). Furthermore, intragenomic rDNA and rRNA sequences are known to have many single-nucleotide polymorphisms (SNPs), with a dominant haplotype and multiple low-abundance variants (amplicon sequence variants, ASVs) in protists, such as ciliates (Gong et al., 2013; Zou et al., 2021), foraminifera (Weber and Pawlowski, 2013; Weber and Pawlowski, 2014), radiolarians (Decelle et al., 2014), and amoebae (Kudryavtsev and Gladkikh, 2017). However, all these previous findings on ribotypes of microbial eukaryotes were obtained under pollutant-free conditions, and the effects of

* Corresponding author at: School of Marine Sciences, Sun Yat-sen University, Zhuhai Campus, Tangjiawan, Zhuhai, 519082, China
E-mail address: gongj27@mail.sysu.edu.cn (J. Gong).

https://doi.org/10.1016/j.crmicr.2026.100643

Available online 10 July 2026

environmental contaminants on these ribotypic attributes in protists remain largely unknown.

Antibiotics are among the most extensively produced and environmentally dispersed pharmaceutical compounds worldwide (Hutchings et al., 2019). Tetracyclines, including oxytetracycline (OTC), are broad-spectrum antimicrobial agents widely applied in human medicine, livestock husbandry, and aquaculture (Daghrir and Drogui, 2013). Concentrations of OTC detected in surface waters typically range from nanograms to a few micrograms per liter, though values exceeding hundreds of micrograms per liter have been recorded in aquaculture effluents and receiving water bodies (Nivedhita et al., 2022). At sub-lethal concentrations, OTC impairs eukaryotic cellular physiology through inhibition of organellar translation, disruption of protein homeostasis, induction of oxidative stress via reactive oxygen species (ROS) accumulation, collectively manifesting as reduced growth rates, cell enlargement, and altered gene expression in protists (Wang et al., 2017; Wang et al., 2020) and microalgae (Guo et al., 2016; Siedlewicz et al., 2020; Wang et al., 2022; Zhong et al., 2021).

Copper (Cu) is a naturally occurring heavy metal that becomes an environmental contaminant through industrial discharge, mining operations, urban stormwater runoff, and the widespread use of Cu-based antifouling paints and pesticides (Flemming and Trevors, 1989). Although Cu is an essential micronutrient at trace concentrations, it functions as a potent toxicant when present in excess (Festa and Thiele, 2011). Dissolved Cu concentrations in unpolluted waters typically range from 0.1 to 10 μg L^{-1}, but can reach hundreds of micrograms per liter in mining-impacted waterways and harbor environments (Falfushynska et al., 2024; Liu et al., 2023). The principal toxic mechanism of Cu involves the generation of hydroxyl radicals via Fenton-like reactions, leading to oxidative damage to lipid membranes, proteins, and nucleic acids (Kim et al., 2011; Somasundaram et al., 2018; Somasundaram et al., 2019). In protists and microalgae, Cu exposure disrupts mitochondrial electron transport, impairs photosynthetic efficiency, interferes with metalloenzyme function, and can trigger programmed cell death (Cid et al., 1996; Hamed et al., 2017; Mu et al., 2017; Shakya et al., 2022).

Sub-lethal exposure of antibiotics or heavy metals is known to elevate mutation rates in bacterial genomes, including rRNA genes, probably due to elevated endogenous oxidative stress, enhanced expression of error-prone DNA polymerases, and a balance with the DNA repair capacity of the bacterial cell (Li et al., 2019; Long et al., 2016; Revitt-Mills and Robinson, 2020; Sigmund et al., 1984; Zhang et al., 2020). Recent studies have suggested that ROS also attack RNA molecules (including rRNA in bacteria and higher organisms) even in a severe manner, causing strand breaks, indels, and mutagenic modification in the nucleobases (Seixas et al., 2022). The most common oxidative modification induced by oxidative stress is the oxidation of nucleobase guanosine into 8-hydroxyguanosine (8-oxo-G), which leads to mispairing with adenine, thus forming G to T (and C to A in reverse complements) transversions during DNA replication and gene transcription (Delaney et al., 2012; Poetsch, 2020). However, little is known about whether the exposure to antibiotics or heavy metals affects the mutations or polymorphisms in nuclear rDNA and rRNA of unicellular eukaryotes (Slaveykova et al., 2016), and to what extent the damaged nucleic acids can be repaired or recovered after stress relief.

In this study, we investigated the effects of sub-lethal OTC and $CuCl_2$ exposure on phenotypic and ribotypic traits of two ciliated protists: the marine heterotrophic species *Euplotes vannus* and the green algae-bearing freshwater species *Paramecium bursaria*. This symbiont-bearing species was selected because, analogous to the sea anemone *Anthopleura elegantissima* harboring symbiotic dinoflagellates (Dykens and Shick, 1982), it possesses an extraordinary capability to quench ROS through its intracellular algal symbionts (Slaveykova et al., 2016), providing a mechanistically informative contrast with the non-symbiotic *E. vannus*. We hypothesized that, after long-term sub-lethal stresses of OTC and $CuCl_2$: (1) the cellular copy numbers of rDNA and rRNA increased with their enlarged cell size and slower growth rate; and (2) more point mutations were induced, resulting in more rDNA and rRNA variants, but to a lesser extent for *P. bursaria*.

Following this research line, we further expected that the effects of copper on intraspecific polymorphisms of 18S rDNA could also apply to the species of broader taxa of eukaryotes. To test the third hypothesis, we leveraged the published data of a recent study using metabarcoding 18S rRNA genes (Corcoll et al., 2019), which showed that $CuCl_2$ stresses decreased the richness of $OTU_{0.97}$ (the operational taxonomic units defined at a 97% sequence identity cutoff) and altered the community structure of microbial eukaryotes in marine biofilms. We calculated the numbers of ASVs per $OTU_{0.97}$ as proxies of rDNA and rRNA sequence diversity per species in the field study, and examined whether they were affected by $CuCl_2$ stress. Our results largely validated these hypotheses, which have important implications for better understanding the molecular microdiversity and distribution of protists along pollutant gradients.

Materials and methods

Cultivation and treatments

P. bursaria strain YD-2010 (GenBank accession No. KC495068.1) was originally isolated from a freshwater pond at the campus of Yantai University, and *E. vannus* isolate WS052 (GenBank accession No. MG603648.1) was collected from the coast of Qingdao, Shandong, China. Both species were identified by light microscopic morphological characterization combined with 18S rRNA gene sequencing, and their identities are further validated from our previous publications (Fu and Gong, 2017; Gong et al., 2014; Zou et al., 2020). Stock cultures of both species were maintained in Petri dishes with sterile freshwater (*P. bursaria*) or artificial seawater (*E. vannus*), supplemented with several rice grains to enrich bacterial prey. To set up growth experiments, ten individual cells were picked from stock culture using a glass micropipette, washed 5 times in sterile medium to minimize contamination, and transferred into Petri dishes each containing 20 mL of sterilized water and 1 mL of heat-killed *Escherichia coli* DH5α suspension (OD_{600} = 0.851). The DH5α strain was selected as a standardized bacterial prey source consistent with protocols established in our previous work (Fu and Gong, 2017; Zou et al., 2020).

The cell cultures of two ciliate species were treated under different levels of antibiotic and heavy metal stresses. Stock solutions of oxytetracycline hydrochloride (OTC·HCl; purity ≥ 99%; Sigma, MO, USA) and cupric chloride ($CuCl_2$; purity ≥ 99%; Sigma, MO, USA) were prepared by dissolving the compound in ultrapure water and added into culture solutions to reach final concentrations at 1, 10, and 20 μg mL^{-1} OTC (equivalent to 2.17, 21.72, 43.44 μM, MW = 460.43 g mol^{-1}) for both two ciliate species; 0.05, 0.1 and 0.2 μg mL^{-1} (equivalent to 0.023, 0.047, and 0.094 μg mL^{-1} Cu, or approximately 0.372, 0.744, and 1.487 μM Cu) $CuCl_2$ for *E. vannus*; and 0.01, 0.02 and 0.05 μg mL^{-1} $CuCl_2$ (equivalent to 0.005, 0.009, and 0.023 μg mL^{-1} Cu, or approximately 0.074, 0.149, and 0.372 μM Cu) for *P. bursaria*. The treatments without adding any of these pollutants were taken as the negative control. In addition, we transferred a few cells from the 30-day treatments at the highest doses of OTC and $CuCl_2$ to fresh media without any pollutants, allowing them to grow and maintain for another month (hereafter referred to as the recovery treatments, or "R0"). For all control and stress treatments, triplicates were set up at a temperature of 21°C in chemostats. An overview of the experimental design is provided in Table S1.

Determination of population growth rate, cell size, and effective concentration

The population growth rate and measurements of cell size were characterized as previously described (Fu and Gong, 2017). Briefly, the population abundance of these ciliates was monitored every 24 h. A 100

μL of cell culture solution was transferred onto a glass slide and fixed with Lugol's solution at a final concentration of 2%. The fixed cells were counted under a stereoscope (XLT-400, Guiguang, China). The natural log cell abundance was plotted against time to generate a growth curve. A linear regression formula for each treatment was derived from the data collected during the logarithmic growth phase, and the slope was taken as the growth rate. The exponentially growing cells were subsampled and fixed, among which 24 individuals were randomly selected to measure the cell width and length under a microscope (Olympus BX51, Tokyo, Japan). The cell volume was calculated assuming an elliptic cylinder shape with a body width to thickness ratio of 3:2 using the following formula: $V = 2\pi ab^2/3$, where V is the cell size (μm^3), a and b are the half of the cell length and width (μm), respectively.

The observed growth rates in the control and stressed treatments were plotted against the tested concentrations of OTC and $CuCl_2$. The effective concentrations required to inhibit growth rate by 10% (EC_{10}) and 50% (EC_{50}) were calculated by regression with the best fits.

Single-cell DNA extraction and cDNA synthesis

Single-cell lysis, DNA extraction, and complementary DNA (cDNA) synthesis were performed following an established single-cell protocol (Zou et al., 2021). In brief, sixteen individual intact cells per treatment were each transferred into a nuclease-free 0.2 mL PCR tube (Axygen Scientific, CA, USA) containing 1 mL of distilled water. Cell membranes were disrupted by adding 2 mL of a lysis solution composed of 0.2% Triton X-100 (Solarbio, Beijing, China) and a recombinant RNase inhibitor (TaKaRa Biomedicals, Japan) at a 19:1 (v/v) ratio. Tubes were gently mixed by flicking, briefly centrifuged, and incubated at room temperature for 10 min. The resulting lysate was partitioned into two fractions: 1 μL for genomic DNA extraction and 2 μL for RNA-based cDNA synthesis. Genomic DNA was isolated using a REDExtract-N-Amp tissue PCR kit (Sigma, St. Louis, MO), with all reagent volumes scaled to 1/50 of the manufacturer's recommended amounts as previously described (Zou et al., 2020).

For cDNA synthesis, residual genomic DNA in the 2 μL RNA fraction was eliminated using the TURBO DNA-free Reagent Kit (Invitrogen). Complete DNA removal was confirmed by PCR amplification of 18S rRNA gene fragments using the eukaryote-specific primers Euk82F (5′-GAADTCGYGAAYGGCTC -3′) and Euk516R (5′- ACCAGACTTGCCCTCC -3′) (Dawson and Pace, 2002; Díez et al., 2001). The DNA-free RNA fraction was then combined with 1 μL random hexamers primers (10mM; Sangon, China) and 1 μL of dNTP mix (10 mM), denatured at 72°C for 3 min, and immediately chilled on ice. Reverse transcription was carried out in a total volume of 12.42 μL containing 4 μL RNA template, 3 μL first-strand buffer, 0.3 μL SuperScript™ III Reverse Transcriptase (Invitrogen), 1 μL dithiothreitol (DTT; 0.1 M), 2 μL betaine (Sigma-Aldrich), 0.12 μL $MgCl_2$ (0.5 M), 1 μL RNase inhibitor (Roche, Mannheim, Germany), and 1 μL DEPC-treated water. Reverse transcription was performed on a thermal cycler (Biometra, Göttingen, Germany) using the following program: 50°C for 90 min, followed by 10 cycles of 55°C for 2 min, and a final inactivation step at 70°C for 15 min. Both purified genomic DNA and synthesized cDNA were stored at -80°C for downstream qPCR quantification and amplicon library preparation.

Quantitative PCR (qPCR)

For quantifying 18S rDNA and cDNA, single cells (n = 16) were subjected to qPCR analysis. The species-specific primers EvQ-F/R (5′-CACTTCTACGGAAGGCAGCA -3′; 5′- TGCCCTCCAATTGTTCCTCG -3′) and PbQ-F/R (5′- AATCCCGACTTACGAAGGGG -3′; 5′-TGTGGTAGCCGTTTCTCAGG -3′) were newly designed to amplify a 144-bp and a 211-bp fragment of the 18S rRNA gene fragments of *E. vannus* and *P. bursaria*, respectively. A series of 10-fold dilutions (10^{-1} to 10^{-10}) of linear DNA fragments was used to generate the standard curves (Gong et al., 2013). A 20-μL reaction solution contained 1 μL of 10 μM primers, 1 μL ROX Reference Dye II, 7 μL SYBR Premix Ex Taq II (Takara, Dalian, China), 10 μL milli-Q water, and 1 μL template. All the qPCR reactions were performed on a 7500 Fast Real-Time PCR System (Applied Biosystems) with the following program: 95°C for 7 min, followed by 45 cycles of 95°C for 30 s, 60°C for 30 s, the data were retrieved at 72°C for both ciliates species; all reactions ended with a melt curve from 60°C to 95°C, with gradually increasing by 0.3°C. The standard curves were generated using $\log_{10}$ copy numbers vs. threshold cycle (Ct). The linear correlation efficiencies (R^2 values) for all assays were greater than 0.998. The amplification efficiency (E) ranged from 81.6% to 90.0%, which was calculated using the formula: $E = (10^{-1/k} - 1) \times 100$, where k is the slope.

High-throughput sequencing and analysis

Genomic DNA and cDNA obtained from single cells of both ciliate species were used to construct amplicon libraries targeting the V1-V4 hypervariable regions of the 18S rDNA and cDNA gene, using the primers Euk82F and Euk516R. A unique 6-bp barcode was incorporated into each primer to enable sample demultiplexing. For each treatment, amplicon libraries prepared from 16 individual single cells were pooled in equimolar ratios prior to sequencing to achieve adequate read depth per treatment. PCR amplification was conducted in a 30 μL reaction volume containing 10 ng of DNA or cDNA, 0.2 μM each primer, and 15 μL of 2 × Phusion high-fidelity PCR master mix (New England BioLabs). Thermal cycling was performed on a T100 thermocycler (Bio-Rad) under the following conditions: initial denaturation at 98°C for 1 min; 30 cycles of denaturation at 98°C for 10 s, annealing at 55°C for 30 s, and extension at 72°C for 30 s, and a final extension at 72°C for 5 min. Amplicon libraries were prepared using the NEBNext Ultra DNA library prep kit according to the manufacturer's instructions. Paired-end sequencing with a read length of 300 bp was performed on MiSeq platforms (Illumina, USA) at Novogene Company (Beijing, China). In total, 36 pooled amplicon libraries comprising rDNA and cDNA-derived pools from both ciliate species across all treatments were sequenced in a single run.

A total of 833,763 and 831,828 raw reads were obtained for the *P. bursaria* and *E. vannus*, respectively (Table S2). To infer amplicon sequence variants, demultiplexed, quality-filtered reads were processed through the DADA2 pipeline (v1.10.1) in R software (v.4.4.0) (Bolyen et al., 2019; Callahan et al., 2016). The primers were trimmed using Cutadapt v1.18 (Martin, 2011), and filtered using *filterAndTrim* of DADA2 with the following parameters: minLen=180, maxEE = c(2,2), maxN = 0, truncQ = 2, rm.phix = TRUE, multithread = TRUE. The filtered sequences were dereplicated using *derepFastq* to generate a unique dataset. The error models were trained using *learnErrors*. Afterward, paired-end reads were merged using the command *mergePairs*, and chimeras and singletons (ASVs contain only one sequence) were eliminated. Finally, 795,547 and 578,633 clean reads remained for *E. vannus* and *P. bursaria* (Table S2).

Taxonomy was assigned against the SILVA_SSU_v138 training set using the *IdTaxa* command of the package DECIPHER v2.14.0 (Murali et al., 2018). The reads assigned to each species were extracted using the software *seqtk*. For treatments of each species, the redundant ASVs were recovered using *deunique.seqs* function of Mothur, based on ASV fasta and sequence count file, then clustered at a series of similarity thresholds (90% to 100%) using UCLUST, and the ribotypic polymorphisms between rDNA and rRNA sequences and across treatments were assessed.

Identification of ribotypic nucleotide polymorphisms

Nucleotide polymorphisms were identified by aligning all rDNA and rRNA (cDNA) reads against the dominant haplotype of each species, which was implemented using Burrows-Wheeler Aligner v.0.7.17 with default parameters (Li and Durbin, 2009). The alignments were

converted into BAM format, sorted, and indexed using SAMtools v.0.1.19 (Li et al., 2009). The ribotypic nucleotide polymorphisms of each species were then called using the *mpileup* function and summarized using an in-house *perl* script (*printBasesBwa2*.pl).

Re-examination of the effect of $CuCl_2$ on ASV richness in a field study

To examine whether the pollutant-induced increases in intragenomic rDNA polymorphism observed in our laboratory cultures could be detected in natural eukaryotic communities, we reanalyzed a publicly available 18S rRNA gene metabarcoding dataset (NCBI BioProject PRJNA496374) from Corcoll et al. (2019). In that study, marine biofilm communities were established on artificial substrata submerged in mesocosms maintained at six $CuCl_2$ concentrations spanning 0 to 10 μM, with three biological replicates per treatment level. Copper was the sole experimentally manipulated variable, though background trace metal and organic contaminant levels in the source seawater were not reported. However, a comparable reanalysis for OTC was not undertaken because no analogous publicly available 18S metabarcoding dataset with a defined OTC concentration gradient in environmental communities was identified.

Microbiome bioinformatics analyses were performed using the DADA2 pipelines (https://benjjneb.github.io/dada2/tutorial.html), with minor modifications. Briefly, adapter and primer sequences were trimmed using Cutadapt v1.18 (Martin, 2011). After a series of data processing steps, including quality filtering, denoising, merging, and removal of chimera and singletons, ASVs were generated using DADA2 (v1.18) (Bolyen et al., 2019). A redundant sequence dataset was recovered based on the FASTA and sequence count file of ASVs using the *deunique.seqs* command in Mothur (v1.46.0). OTUs were clustered at 97% sequence similarity using UCLUST, and the OTU table was rarefied to 41,000 reads per sample to standardize sequencing depth across treatments. Taxonomy was assigned using the Protist Ribosomal Reference database (PR^2) (Guillou et al., 2013). The 15 most abundant protistan OTUs were selected, and their sequences were extracted separately for downstream analysis. $OTU_{0.97}$ and ASV tables were generated at a 97% and 100% similarity thresholds, respectively. $OTU_{0.97}$ does not correspond to a biological species, but may be comparable to morphospecies-level variation in small subunit RNA genes, as commonly assumed in traditional microbial community profiling studies. We therefore used the number of ASVs per $OTU_{0.97}$ as an analogous indicator of intraspecific rDNA polymorphism. ASV richness per $OTU_{0.97}$ was estimated by repeated subsampling (50 iterations; Table S3) to enable robust comparisons among $CuCl_2$ treatments. The same approach was applied at the kingdom and phylum levels to assess the taxonomic generality of pollutant-induced ASV richness increases.

Statistical analysis

Differences in growth rate, cell size, rDNA, and rRNA copy number among different OTC and $CuCl_2$ treatments were assessed by One-way ANOVA (with LSD *post hoc* test). Differences in ASV number per $OTU_{0.97}$ among $CuCl_2$ concentration groups were evaluated by the same approach, with Student's *t*-test used for pairwise comparisons between two groups. Normality and homogeneity of variances were verified using the Shapiro-Wilk and Levene's tests, respectively. Pearson's correlation analysis and linear regression analysis were performed to explore the relationships among growth rate, cell size, and rDNA and rRNA copy numbers. Differences in scaling slopes of the allometric relationship between cell volume and cellular rDNA copy number, with and without the pollutant-stressed dataset, were tested by analysis of covariance (ANCOVA). All statistical analyses were executed using SPSS v.20.0 (SPSS, Chicago, IL, USA). All figures were generated with ggplot2 (v. 4.0.0) in R.

Results

Variations in growth rate and cell size with OTC and $CuCl_2$ concentrations

In general, both OTC and $CuCl_2$ showed an inhibitory effect on the growth of the tested ciliates (Fig. 1A-D, Fig. S1). The two ciliates showed different tolerance to OTC and $CuCl_2$, since the EC_{10} and EC_{50} of OTC for *E. vannus* were 0.13 and 8.35 μg mL^{-1}, which were lower than those for *P. bursaria* (0.40 and 55.26 μg mL^{-1}). Nevertheless, the EC_{10} and EC_{50} of $CuCl_2$ were higher for *E. vannus* (0.02 and 0.15 μg mL^{-1}) than for *P. bursaria* (0.003 and 0.026 μg mL^{-1}). Relative to the control, the growth rate of both *E. vannus* and *P. bursaria* gradually decreased with the increasing dose of OTC and $CuCl_2$ (Fig. 1A-D). Following re-inoculating the high-dose-treated cells into an OTC-free medium and maintained for another month (i.e., the R0 treatment), *E. vannus* and *P. bursaria* grew still more slowly than the control, with only 79% and 83% of the growth rate being recovered relative to the control (Fig. 1A-B). So were the populations recovered from $CuCl_2$ treatments, which reached 80% and 60% growth rate of the control (Fig. 1C-D).

The cell volume of two ciliate species tended to increase with the concentrations of OTC and $CuCl_2$ (ANOVA, $P < 0.001$; Fig. 1E-H). In addition, the cells of both species in the recovered treatments remained consistently and significantly larger than those in the control ($P < 0.05$; Fig. 1E-H), demonstrating that there was a lasting effect of pollutants on cell size.

Responses of cellular rDNA and rRNA copy numbers to stresses

The qPCR assays showed that both rDNA and rRNA (cDNA) copy numbers per cell increased with the dose of OTC and $CuCl_2$ in most cases (Fig. 2). Under no stress, *E. vannus* and *P. bursaria* had $(2.25 \pm 0.07) \times 10^5$ and $(3.47 \pm 0.12) \times 10^5$ rDNA copies $cell^{-1}$, which were about 4.8% and 3.8% of their per-cell rRNA transcript abundances, respectively. In both OTC and $CuCl_2$ treatments of *P. bursaria*, the per-cell rDNA and rRNA copy numbers consistently peaked at the highest doses, exhibiting an increase of about 30% and 35% (in the OTC treatment) and 82% and 104% (in the $CuCl_2$ treatment) (Fig. 2B, D). Similar patterns occurred in the $CuCl_2$ treatments (Fig. 2C), but not in the OTC treatments, of *E. vannus* (Fig. 2A), in which the per-cell rDNA copy number was exceptionally lowered at both medium and high doses ($P < 0.05$), whereas the per-cell rRNA transcript abundance remained at much higher levels (Fig. 2A). Re-inoculation in pollutant-free media usually led to recovery of rDNA copy numbers in single cells (Fig. 2A-C), but not for the $CuCl_2$-treated *P. bursaria* (Fig. 2D). In contrast, the rRNA transcript copies in the recovery treatments of these two species remained at higher levels, relative to those in the control (Fig. 2A-D).

The cellular concentration of both rDNA and rRNA copies was significantly affected under the pollutant stresses (ANOVA, $P < 0.001$; Fig. 2E-L). The cellular concentrations of rDNA were consistently the lowest at the highest doses of the pollutants, and never recovered to comparable levels observed in the control after recovery treatments (Fig. 2E-H). Nevertheless, the cellular concentrations of rRNA transcripts were the highest at low or medium doses (Fig. 2I-K), except for that in the control treatment of $CuCl_2$ for *P. bursaria* (Fig. 2L). Likewise, recovery treatments failed to bring the altered rRNA concentrations to the levels of the control (Fig. 2I-L).

The ratio of rRNA to rDNA copy numbers in both species was highly and significantly affected by OTC (ANOVA, $P < 0.001$), but not significantly affected by $CuCl_2$ treatments ($P > 0.30$), suggesting a differential effect of these two pollutants on the expression level of rRNA genes (Fig. 2M-P). The rRNA: rDNA ratio at a single-cell level ranged from 9 to 107 in *E. vannus*, and from 12 to 58 in *P. bursaria* across all the treatments. Compared with the control, higher ratios were often identified in an OTC treatment ($P < 0.05$; Fig. 2M-P). However, the ratios remained higher in the recovery treatments than in the control (Fig. 2M-O), except for $CuCl_2$-treated *P. bursaria*, which had a similar rRNA: rDNA copy

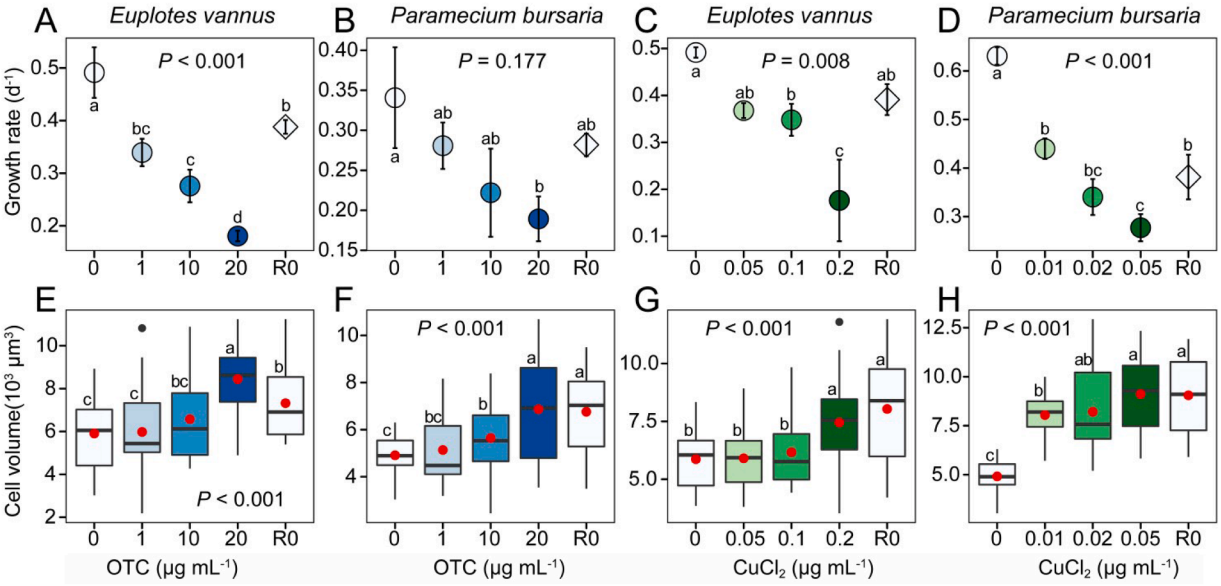

Fig. 1. Phenotypic changes of *Euplotes vannus* and *Paramecium bursaria* under oxytetracycline (OTC) and $CuCl_2$ treatments. (A-D) Maximum growth rates. (E-H) Cell volume. Group differences were analyzed using one-way ANOVA. Treatments not sharing any lowercase letters are significantly different ($P < 0.05$). "R0" denotes the recovery treatment, in which a few cells were transferred from the highest concentration of OTC or $CuCl_2$ treatments and re-cultured in pollutant-free medium.

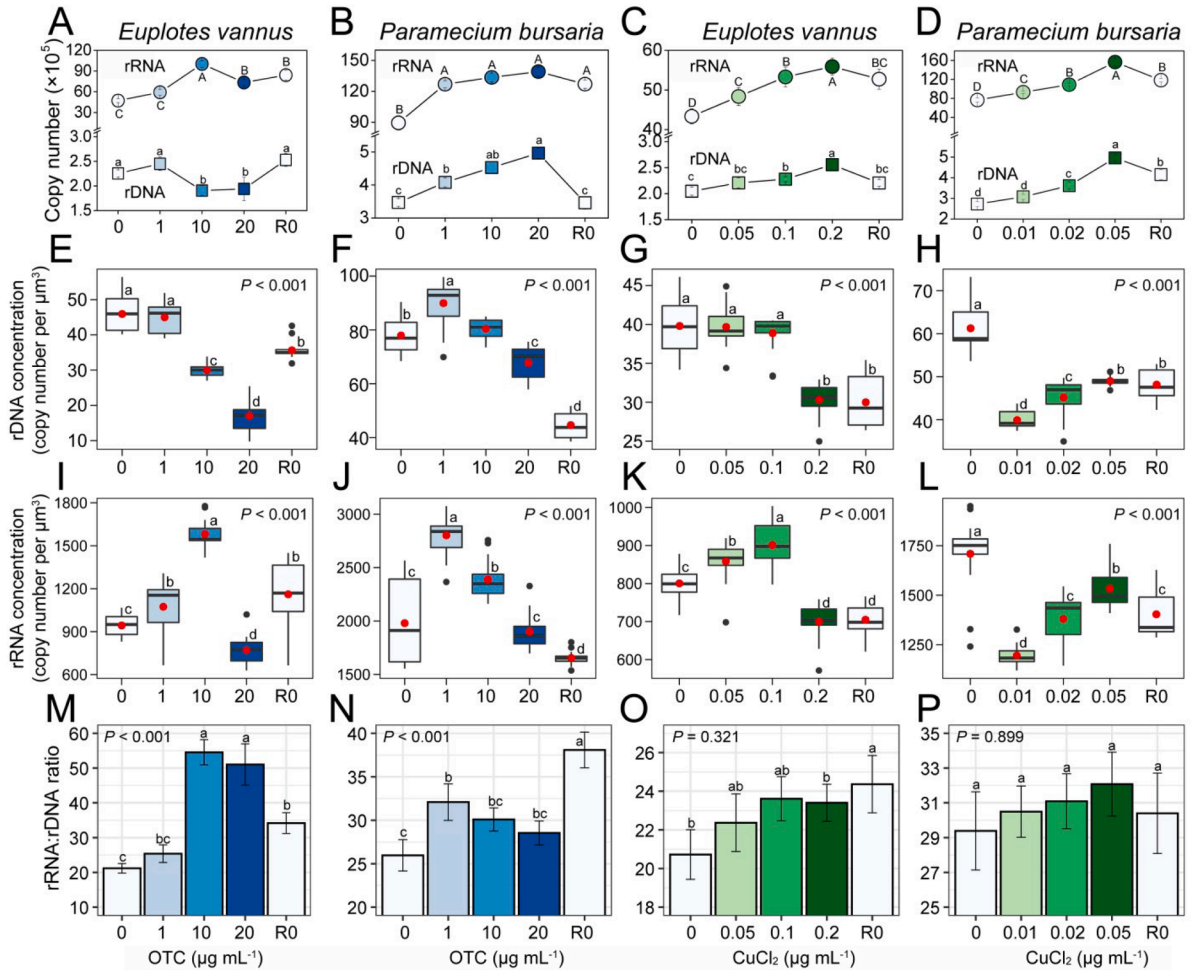

Fig. 2. Genotypic variations in *Euplotes vannus* and *Paramecium bursaria* along oxytetracycline (OTC) and $CuCl_2$ gradients. (A-D) 18S rDNA and rRNA transcript copy numbers per cell. (E-H) 18S rDNA copy numbers per unit cell volume. (I-L) 18S rRNA transcript copy numbers per unit cell volume. (M-P) rRNA-to-rDNA copy number ratio. "R0" indicates the recovery treatments. Treatments not sharing any lowercase or uppercase letters are significantly different ($P < 0.05$).

number ratio in the control and the recovery treatment (Fig. 2P).

Relationships between cell volume, per-cell rDNA and rRNA copy numbers, and growth rate

Linear regression analysis revealed no relationships between per-cell rDNA, rRNA copy numbers, and cell volume (CV) of *E. vannus* and *P. bursaria* across all treatments ($R^2 < 0.06$; $P > 0.33$; $n = 20$; Fig. 3A, insert). In combination with previous data of several ciliate species (Fu and Gong, 2017; Zou et al., 2021), the power-law scaling relationships between cell volume and cellular rRNA transcript abundance were well established, regardless of the pollutant-stressed data being taken into account ($R^2 = 0.98$, $P < 0.001$, $n = 45$) or not ($R^2 = 0.98$, $P < 0.001$, $n = 29$; Fig. 3A). However, the allometric relationship between CV and cellular rDNA copy number remained statistically significant regardless of whether pollutant-stressed data were excluded ($R^2 = 0.53$, $P = 0.008$, slope = 0.452, 95% CI: 0.151-0.753, $n = 12$) or included ($R^2 = 0.34$, $P = 0.001$, slope = 0.564, 95% CI: 0.247-0.879, $n = 28$; Fig. 3A; Table S4). ANCOVA confirmed that the two datasets did not differ significantly in scaling slope ($F = 0.479$, $P = 0.495$), indicating that pollutant stress did not fundamentally alter the form of the allometric relationship.

In combination with temperature, CV, and ribotypic traits (rDNA and rRNA copy number per cell, and rRNA: rDNA ratio) obtained in previous and this study, were used for fitting growth rate (Fig. 3B, C; Table S4). Overall, per-cell rDNA CN turned out to be the best variable (adj. $R^2 \geq 0.85$; Fig. 3B, C), followed by rRNA: rDNA ratio ($0.80 \geq$ adj. $R^2 \geq 0.60$), and CV or rRNA copy number per cell the least ($0.15 \geq$ adj. $R^2 \geq 0.45$; Table S4). Excluding the pollutant-stressed data of *E. vannus* and *P. bursaria* from the regression model slightly improved predictive performance (adj. $R^2 = 0.90$, $n = 16$) compared with including them (adj. $R^2 = 0.85$, $n = 32$), and the slope of growth rate versus rDNA content became marginally less steep (-0.488 vs. -0.528) (Fig. 3B, C).

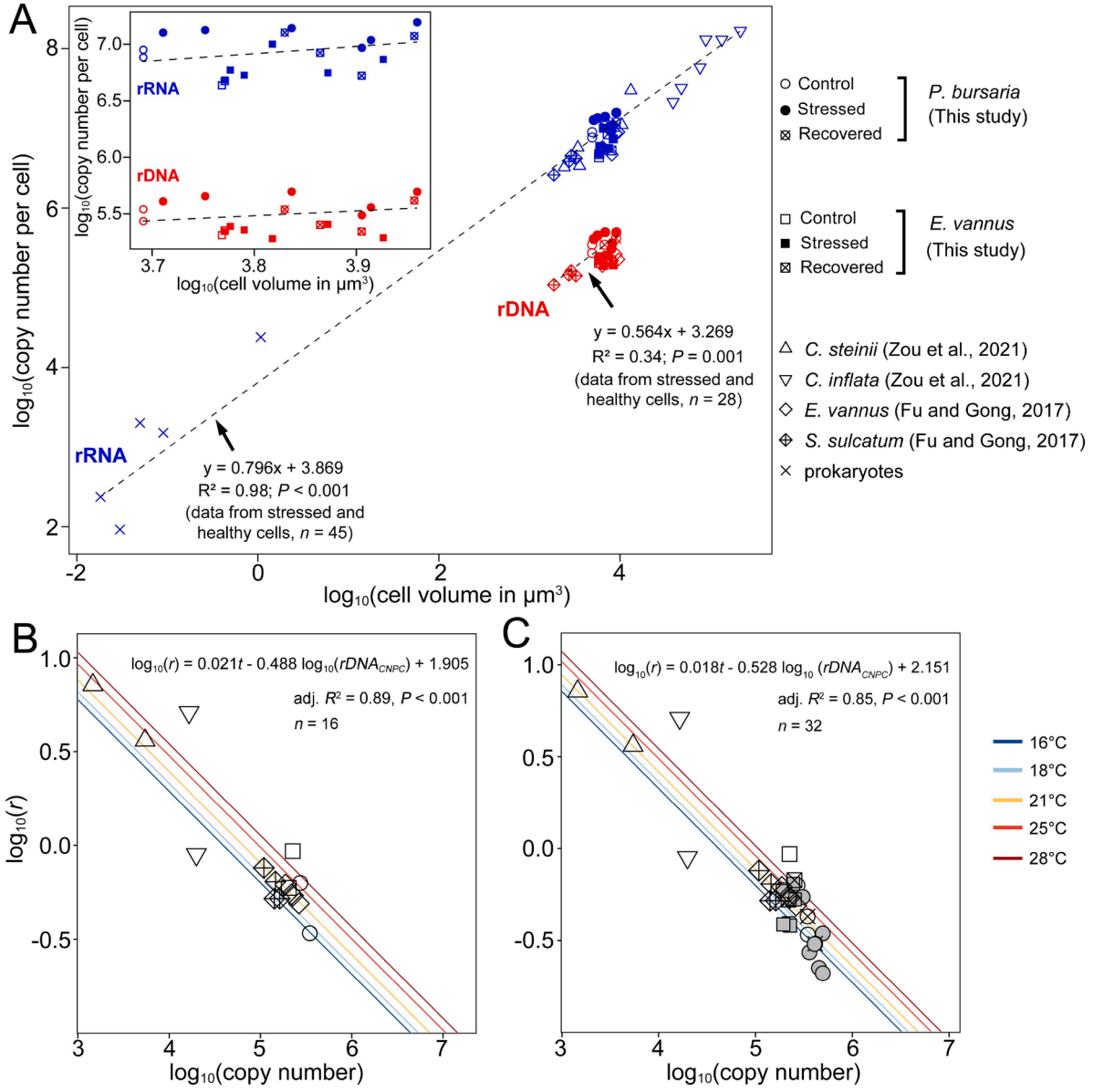

Fig. 3. Allometric relationships among ribotypic traits, growth rates, and cellular features. (A) rDNA (red) and rRNA (blue) copy numbers in two ciliates exposed to oxytetracycline (OTC) and $CuCl_2$ showed no significant correlation with cell volume (inset). However, strong scaling relationships emerged when data from diverse sources were incorporated: two *Colpoda* species across life stages [1], *Euplotes vannus* and *Strombidium sulcatum* reared at different temperatures [2], and five prokaryotic species [3-6]. (B) Maximum growth rates (r) of *P. bursaria, E. vannus, C. steinii, C. inflata, E. vannus*, and *S. sulcatum* are well predicted by rDNA copy number per cell (*CNPC*) and temperature (t). (C) Prediction accuracy declines when stressed treatments are included.

Intra-individual sequence polymorphism of rRNA genes and transcripts

Across all the treatments, there was a single dominant ASV in *E. vannus* and *P. bursaria*, accounting for a generally high percentage ranging from 75% to 100% and 96% to 100%, respectively (Fig. S2). Other ASVs were mostly rare, with the SNP sites almost randomly distributed in the amplified fragments of 18S rRNA gene of *E. vannus*, and relatively clustered in several sub-regions in those of *P. bursaria* (Fig. 4A). In contrast, the rRNA (cDNA) sequences had more SNP sites than the genes, which was especially true for *P. bursaria* (Fig. 4A). By

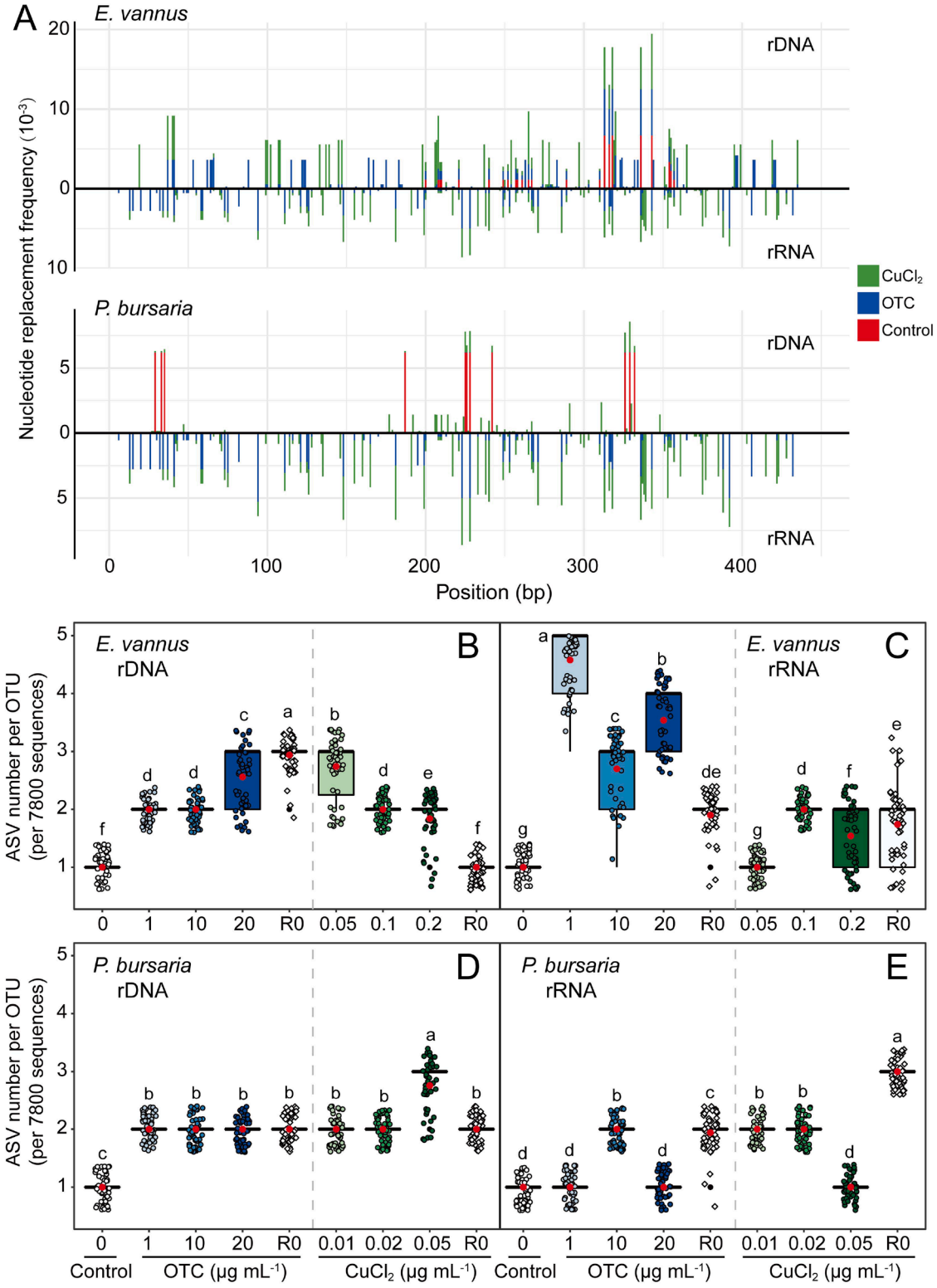

Fig. 4. Genotypic variations in *Paramecium bursaria* and *Euplotes vannus* under oxytetracycline (OTC) and $CuCl_2$ exposure. (A) Intra-individual rDNA and rRNA sequence polymorphisms. (B-E) Number of ASVs per OTU. OTUs were defined at a 97% sequence identity cutoff. "R0" indicates the recovery treatment. Treatments not sharing any lowercase letters are significantly different ($P < 0.05$).

randomly subsampling 7800 reads for 50 times, the numbers of ASVs were estimated to be 2 to 5 in the OTC and $CuCl_2$ treatments of both *E. vannus* and *P. bursaria*, which were significantly higher than those (1 ASV) in the controls ($P < 0.05$; Fig. 4B-E). Stress relieving did not lead to a reduction of ASV richness of both rRNA genes and transcripts, but mostly remained higher in the recovery treatments than the control, except for the rDNA of *E. vannus* treated with $CuCl_2$ (Fig. 4B).

We observed small but statistically significant shifts in GC content of 18S rDNA and rRNA sequences in *E. vannus* and *P. bursaria* following sublethal exposure to OTC and $CuCl_2$ (Fig. 5). In rDNA, OTC significantly reduced GC content relative to controls in both species ($P < 0.05$), whereas $CuCl_2$ induced the opposite response, increasing GC content most notably at intermediate concentrations (0.1 μg mL^{-1}). In recovery (R0) treatments, rDNA GC content remained significantly lower than in controls for both species ($P < 0.05$; Fig. 5). For rRNA transcripts, OTC increased GC content in *E. vannus* but decreased it in *P. bursaria*, while $CuCl_2$ exerted negligible effects on *E. vannus* rRNA GC content yet markedly reduced it in *P. bursaria* (Fig. 5). These divergent patterns suggest stressor-specific and species-dependent influences on ribosomal sequence composition under sublethal chemical stress.

Variations in ASV number per OTU in microbial eukaryotic communities under $CuCl_2$ exposure

We re-analyzed the metabarcoding data of 18S rRNA genes of eukaryotic communities in marine biofilms and soils along $CuCl_2$ and antibiotic gradients (Corcoll et al., 2019). Of the most abundant 15 protistan OTUs in the biofilm communities, the number of ASV per OTU varied significantly across the $CuCl_2$ gradient (from 0 to 10 μM) or between two concentrations (ANOVA or *t*-test, $P < 0.01$; Fig. 6), with usually 1 ASV per OTU in the control, and a comparable or higher (e.g., up to 5 or 6 ASVs in the OTUs closely related to a diatom species, *Phaeodactylum tricornutum*) number of ASV per OTU in a stressed treatment, except for three OTUs (Fig. 6). Of protistan OTUs in general and within a (16 out of 20) major protistan taxa (e.g., Bacillariophyta, Cercozoa, Chlorophyta, Ciliophora, Dinoflagellata, and Haptophyta; see Table S3), the average number of ASVs per OTU was dependent on the applied dose of $CuCl_2$ (ANOVA, $P < 0.05$), and tended to increase with the dose of $CuCl_2$, or peaked at an intermediate dose of the pollutant (Fig. 7A; Table S3). However, metazoan and fungal OTUs usually had fewer ASVs under highly stressed conditions (Fig. 7B, C). Exposure to $CuCl_2$ generally increased ribosomal GC content across lineages ($P \leq 0.037$; Fig. S3). Protists and metazoa showed higher GC content in polluted versus unpolluted conditions, with exceptions at 1.78 μM and 0.06μM $CuCl_2$, respectively (Fig. S3AB). Fungi exhibited pronounced GC elevation at 10 μM relative to 1.78 μM $CuCl_2$ (Fig. S3C).

Discussion

Sublethal exposure to toxic pollutants has been intensively studied through phenotypic and genotypic responses in eukaryotes, with emphasis typically placed on functional genes involved in detoxification, repair, and metabolism. In contrast, the quantitative traits of 18S rRNA genes were more or less overlooked in previous toxicological research, probably because they are highly redundant in eukaryotic genomes and their expressions are often considered stable (housekeeping). Our single-cell analyses of *E. vannus* and *P. bursaria* demonstrate for the first time that the sublethal doses of an antibiotic and a heavy metal significantly alter cellular contents, expression, and nucleotide polymorphisms of 18S rRNA genes of protists, which sheds new light on the biological response and adaptation of single-celled eukaryotes to toxic stresses.

The changes in rDNA and rRNA cellular contents under sublethal exposure were not solely accounted for by cell size variation

Our study demonstrates that cellular contents of rDNA and rRNA in the ciliates *E. vannus* and *P. bursaria* vary with antibiotic and heavy metal stresses, providing additional evidence for the dynamic nature of these biomolecules in single-celled eukaryotes (Fu and Gong, 2017; Zou et al., 2021). The observed increase in cellular rDNA and rRNA contents (Fig. 2A-D) are consistent with the phenotypic responses to pollutant stresses of these two species (growth inhibition and cell enlargement), which were consistent with the previously documented for a range of protistan species (Kim et al., 2018; Wang et al., 2017; Wang et al., 2020; Zhong et al., 2021). Given that copy numbers scale negatively with

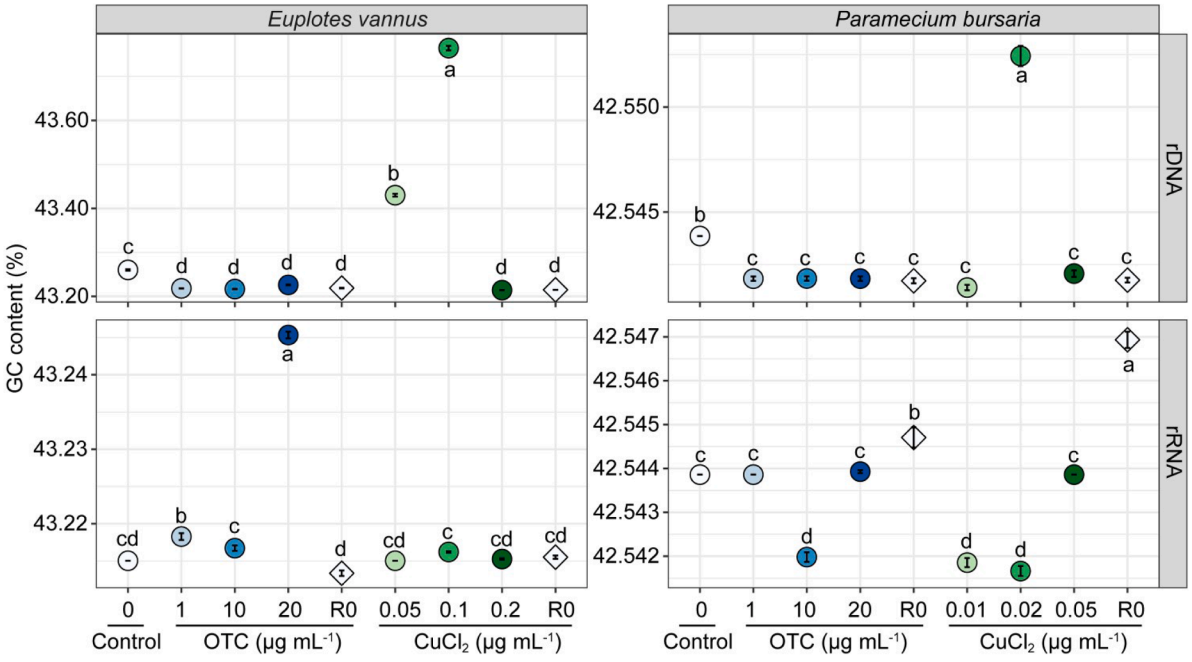

Fig. 5. GC content variations in of 18S rDNA and rRNA transcripts in single cells of *Euplotes vannus* and *Paramecium bursaria* under oxytetracycline (OTC) and $CuCl_2$ treatments. "R0" indicates the recovery treatment. Treatments not sharing any lowercase letters are significantly different ($P < 0.05$).

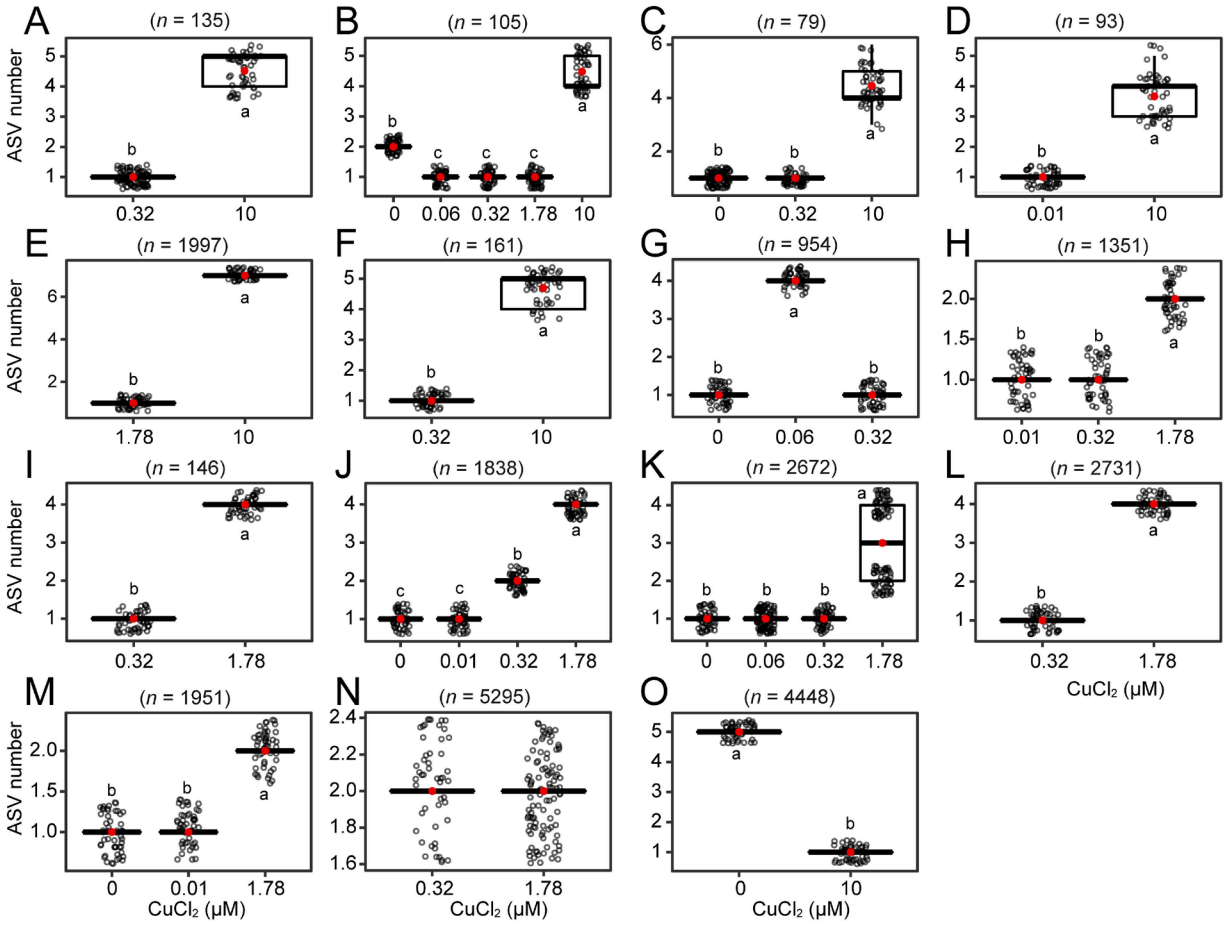

Fig. 6. Variations in amplicon sequence variant (ASV) number per operational taxonomic unit (OTU) among the top 15 dominant protistan OTUs in marine biofilms across $CuCl_2$ gradients (0-10 μM) [7]. One-way ANOVA with LSD post hoc test was used to assess differences in ASV number per OTU among $CuCl_2$ concentration groups, and Student's t-test was applied for pairwise comparisons. (A-F) Six diatom OTUs affiliated with *Phaeodactylum tricomutum*. (G) A diatom OTU affiliated with *Nitzschia* sp. (H) A Raphid-pennate OTU (diatom). (I) A *Paraflabellula hoguae* OTU (Lobosa). (J-O) Six OTUs of *Labyrinthula diatomea* (Labyrinthulomycetes). OTUs were defined at a 97% sequence identity cutoff. Treatments not sharing any lowercase letters are significantly different ($P < 0.05$). Comparisons were based on even sampling effort of sequence numbers (*n*).

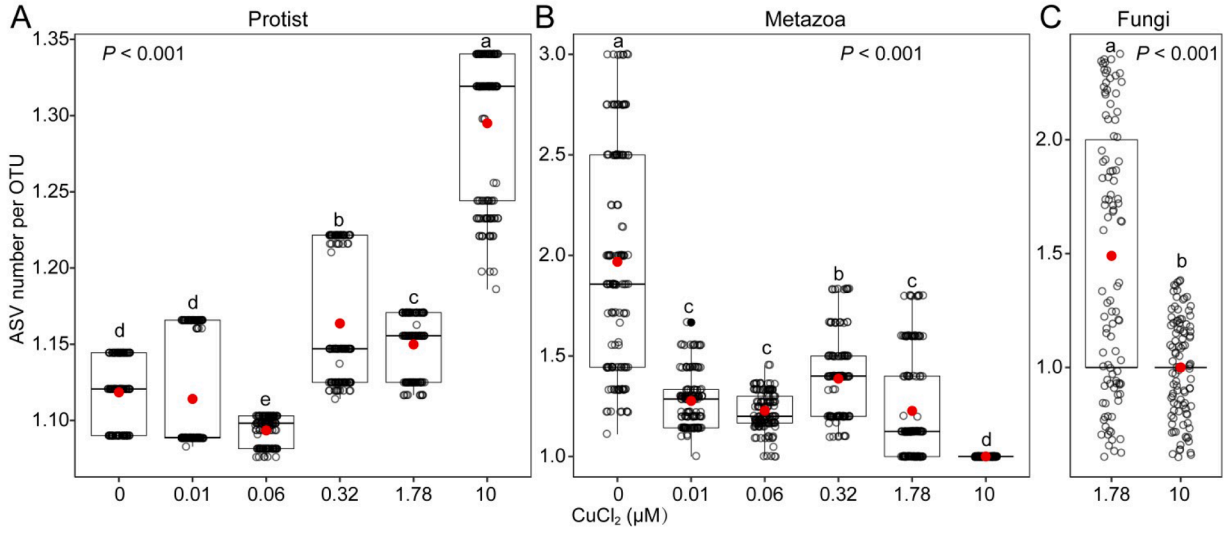

Fig. 7. Changes in amplicon sequence variant (ASV) number per operational taxonomic unit (OTU) of eukaryotic groups in marine biofilms in response to $CuCl_2$ stress [7]. (A) Protists. (B) Metazoa. (**C**) Fungi. OTUs were defined at a 97% sequence identity cutoff. One-way ANOVA with LSD *post hoc* test was applied to assess differences, and Student's *t*-test was used for pairwise comparisons. Treatments not sharing any lowercase letters are significantly different ($P < 0.05$).

growth rate and positively with cell volume (Fu and Gong, 2017; Zou et al., 2021), it is not surprising that both stressors increased per-cell

rDNA and rRNA copy numbers in *E. vannus* and *P. bursaria* in the present study.

What was unexpected was that there were disproportionately higher cellular rRNA concentrations (rRNA copies per unit volume) when the cells were facing OTC and $CuCl_2$ stress, compared with the control (Fig. 2I–K), suggesting that changes in cell size alone are insufficient to account for the unusually high rRNA concentrations. We interpret this "extra" ribosomal output as a stress-specific compensatory response: oxidative damage to existing ribosomes and ribosomal proteins, known to impair translation efficiency and fidelity (Shcherbik and Pestov, 2019; Simms and Zaher, 2016), triggers upregulation of ribosomal biogenesis to maintain adequate protein synthesis capacity. The excess rRNA likely supports not only replacement of damaged components but also elevated production of stress-response proteins (e.g., antioxidants and repair enzymes) needed to counteract ROS-mediated damage.

Divergent toxicological effects of OTC and $CuCl_2$ on ribotypic variation

Although both stressors increased per-cell rDNA and rRNA copy numbers in *E. vannus* and *P. bursaria*, they elicited markedly different effects on the rRNA: rDNA ratio (Fig. 2M-P). OTC produced a substantial elevation in this ratio, whereas $CuCl_2$ had minimal impact. The divergence may reflect distinct mechanistic pathways of toxicity. The tetracycline antibiotic inhibits protein synthesis by binding the 30S ribosomal subunit (albeit weakly in eukaryotes) and can disrupt organellar translation in protists, triggering compensatory upregulation of rRNA transcription to restore translational capacity (Chopra et al., 1992). In contrast, copper primarily induces mitochondrial dysfunction and cuproptosis via ROS generation and TCA cycle disruption (Hosseini et al., 2014; Tsvetkov et al., 2022), leading to proportional increases in both rDNA amplification and rRNA synthesis without preferential transcriptional upregulation. Both stressors, however, likely converge on oxidative stress as a common driver, with ROS-mediated damage to existing ribosomes necessitating excess rRNA production for repair, assembly, or replacement (Shcherbik and Pestov, 2019; Simms and Zaher, 2016; Willi et al., 2018). Evidence from model systems further supports this view: rDNA copy-number variation buffers translational demand under stress in yeast (Thornton et al., 2024), while oxidative stress induces rDNA instability and amplification in human and plant cells exposed to pollutants (e.g., PAHs and metals) (Wang et al., 2023). In protists, our results suggest analogous adaptive plasticity, where elevated ribosomal content may mitigate translation defects and support the synthesis of stress-response proteins, though at the cost of persistent cellular enlargement and reduced growth even after stressor removal.

Pollutant-induced intragenomic divergence in ribosomal RNA gene and rRNA transcripts

Although antibiotic-induced mutagenesis has been well documented for ribosomal RNA genes or whole genomes of bacteria and for eukaryotic plastid and mitochondrial organelles of bacterial origin (e.g., Brain et al., 2008; Prezant et al., 1993), the effects of antibiotics on nuclear rRNA genes of eukaryotes remain poorly understood. Likewise, few studies have focused on heavy metal effects on rRNA genes. Our single-cell sequencing revealed significantly elevated ASV richness in both rDNA and rRNA under OTC and $CuCl_2$ exposure, providing evidence that antibiotics and heavy metals may induce mutagenesis of eukaryotic ribosomes. Systemic oxidative stress (SOS) responses and DNA repair inhibition may be involved in this pollutant-induced mutagenesis (Morales et al., 2016; Zhang et al., 2020), with oxidative stress amplifying transcriptional or post-transcriptional errors beyond genomic mutations (Poetsch, 2020).

Furthermore, regarding the origin of high intragenomic polymorphism of rDNA in eukaryotes (Gong et al., 2013; Weber and Pawlowski, 2014), which are known as multi-copy gene clusters subject to concerted evolution (Dover, 1982), many hypotheses (e.g., transition stage, pseudogenes, interspecific hybridization, and genomic organization) have been discussed (Weber and Pawlowski, 2014). Our experiments showed for the first time elevated sequence polymorphisms and altered copy numbers of rDNA and their transcripts, which did not fully recover after stress relieving. A possible explanation is residual pollutant carryover (even after one month) and persistent physiological damage. These scenarios may occur in macro-organisms (e.g., fish, mollusks) with relatively long lifespans (several years), but they are less likely for unicellular ciliated protists. According to the growth rates we calculated for the recovery treatments (0.27 d^{-1} to 0.4 d^{-1}; Fig. 1A-D), each cell divides every 2.5 - 3.7 days. This means that inoculation of a single cell in pollutant-free medium will produce approximately 8.1 - 12.0 generations over one month, ideally yielding a population of 276 - 4096 cells. Even if the pollutants were carried over from generation to generation and never released from the cells, their intracellular concentration would be diluted 276- to 4096-fold. Additionally, we picked single cells rather than whole populations for sequencing, which prevents interpreting the higher polymorphism levels as an accumulative result from all individuals within the population. The same argument applies to physiological damage. Therefore, it is unlikely that an almost pollutant-free culture would remain toxic for approximately 10 generations, and our results on recovery treatment suggest a genetic imprint on rRNA genes by sublethal stress, the molecular and genetic mechanisms of which remain to be elucidated.

Sublethal exposure to OTC and $CuCl_2$ induced small but significant, dose-dependent shifts in 18S rDNA and rRNA GC content in *E. vannus* and *P. bursaria* at the single-cell level (Fig. 5), paralleling field observations of generally elevated ribosomal GC content across protistan, metazoan, and fungal lineages under $CuCl_2$ exposure (Fig. S3). However, the two stressors drove GC content in opposite directions: OTC reduced rDNA GC content, consistent with 8-oxo-dG-driven G-to-T transversions that represent the canonical oxidative mutagenic signature (Hahm et al., 2022), whereas $CuCl_2$ elevated GC content, suggesting distinct lesion spectra or differential DNA repair pathway activation. These opposing shifts indicate that OTC and $CuCl_2$ do not act solely through a shared ROS-mediated mutagenic pathway, despite both inducing oxidative stress. Nonetheless, the general trend toward elevated GC content under pollutant stress aligns with broader environmental selection for GC-rich genomes in prokaryotes and eukaryotes, which enhances DNA thermal stability, transcriptional robustness, and resistance to oxidative damage (Basak and Ghosh, 2005; Matallana-Surget et al., 2008; Reichenberger et al., 2015). Elevated GC content may thus represent an adaptive mechanism to maintain genome integrity and transcriptional fidelity under chronic antibiotic exposure (Weissman et al., 2019), particularly in symbiont-bearing species such as *P. bursaria* that possess inherent ROS-quenching capacity (Summerer et al., 2009).

Our single-cell analysis provides evidence that sublethal pollutant stress enhances intragenomic sequence diversity of 18S rRNA genes. Although classical genotoxicity essays (e.g., DNA strand break quantification) were not conducted, the dose-dependent, persistent, and cross-species increases in rDNA polymorphism are consistent with pollutant-induced mutagenic pressure on ribosomal gene loci. By analyzing a published dataset, we found the average number of ASVs per OTU_{97} increased significantly with $CuCl_2$ concentration across multiple protistan taxa, indicating that the genotoxicity of the copper on rRNA gene sequences are exerted not only on ciliates, but likely influences broader eukaryotic taxa in the environment. This finding is of ecological and toxicological importance.

The pollutant-induced rDNA mutagenesis documented here may have lasting evolutionary consequences for ciliate populations. The incomplete reversal of elevated ASV richness following stressor removal suggests that a proportion of induced rDNA variants may be stably inherited across cell generations, potentially contributing to standing genetic variation in natural populations. Under repeated or chronic pollutant exposure, such variants could serve as raw material for

evolutionary adaptation, particularly given the widespread and persistent nature of anthropogenic contamination in aquatic environments. Environmental contaminants may thus function as ecological filters that selectively favor genotypes with enhanced rDNA stability or greater ribosomal gene plasticity. Our data further reveal marked interspecific differences in pollutant tolerance: *P. bursaria* was substantially more resistant to OTC ($EC_{50} = 55.26$ μg mL^{-1}) than *E. vannus* ($EC_{50} = 8.35$ μg mL^{-1}), an asymmetry that may partly reflect the ROS-quenching capacity of its intracellular algal symbionts. More broadly, differential sensitivities among protistan taxa to specific pollutants are likely to reshape community composition in contaminated environments, with cascading consequences for microbial food web structure and ecosystem processes such as nutrient cycling and carbon flux.

Previous studies have typically used mock communities of phylogenetically diverse species to evaluate the effect of GC content on sequencing results, demonstrating PCR bias against GC-rich species (Laursen et al., 2017; Qin et al., 2023). The tested species were affiliated with diverse bacterial phyla, with GC content ranging widely from 30% to 70%. The authors attributed this bias to differences in primer affinity and annealing temperatures, leading to variable amplification efficiencies (Laursen et al., 2017; Qin et al., 2023). In contrast to these experimental settings, our re-analysis of the field data focused on sequence variation within a single $OTU_{0.97}$, which may be comparable to a morphospecies level as traditionally assumed in community profiling studies. The range of rDNA CG content within an OTU (or a morphospecies) is relatively narrow (for example, up to 0.5% for *E. vannus* and 0.01% for *P. bursaria*; Fig. 5). We therefore believe that these highly similar DNA sequences pose minimal problems regarding primer affinity and annealing temperature. Our finding that the polymorphisms increase under OTC and $CuCl_2$ stress, derived from single-cell analysis of *E. vannus* and *P. bursaria* in the present study, further supports the results of our field data re-analysis.

Nowadays, amplicon sequence variants have been increasingly used for characterizing prokaryotes and microeukaryotes in various systems (e.g., He et al., 2024; Zou et al., 2024). Our findings in this study indicate that many pollutant-induced 18S rRNA gene sequence variants from a species, even an individual protistan cell, could be recovered in metabarcoding studies. When interpreting the ASV-based microbial diversity patterns, the potential of ASV richness inflation and increases of per-cell rDNA abundance due to genotoxicity of pollutant stress should be borne in mind.

Consistently higher intragenomic polymorphisms were observed in rRNA transcripts than in rDNA across all treatments, a finding consistent with our previous single-cell analysis (Zou et al., 2021). rRNA-based metabarcoding is commonly applied to characterize active microbial communities. Our single-cell-based finding suggests that rRNA-derived libraries may yield higher apparent richness of active microbes than rDNA-derived libraries. While this pattern may partly reflect genuine transcriptional polymorphisms or post-transcriptional RNA editing, contributions from reverse transcription errors, RNA degradation, or cDNA synthesis artifacts cannot be excluded. Future studies incorporating spike-in controls of *in vitro* transcribed RNA with known sequences, or employing unique molecular identifiers, would estimate the percentages of sequencing accuracy. To practically distinguish accurate sequences from artifacts, we recommend an integrative approach combining both rDNA and rRNA sequencing, enabling cross-referencing of the two datasets to identify and exclude artifactual ASVs (Deng et al., 2024; Yu et al., 2025).

Author contributions

Conceptualization, Jun Gong; formal analysis, Songbao Zou, Rao Fu, Huiwen Deng; writing—original draft preparation, Songbao Zou, Julin Yuan; writing—review and editing, Songbao Zou, Jun Gong. All authors commented on previous versions of the manuscript, and read and approved the final manuscript.

Ethics statement

No animal or human research was involved in this study.

Funding

This work was supported by the Zhejiang Provincial Natural Science Foundation of China (Grant No. LQN25C190014) and National Natural Science Foundation of China (No. 42376086).

Declaration of competing interest

The authors declare that they have no known competing financial interests or personal relationships that could have appeared to influence the work reported in this paper.

Supplementary materials

Supplementary material associated with this article can be found, in the online version, at doi:10.1016/j.crmicr.2026.100643.

Data availability

https://www.ncbi.nlm.nih.gov/bioproject/PRJNA692502

References

Basak, S., Ghosh, T.C., 2005. On the origin of genomic adaptation at high temperature for prokaryotic organisms. Biochem. Biophys. Res. Commun. 330 (3), 629–632. https://doi.org/10.1016/j.bbrc.2005.02.134.

Bolyen, E., Rideout, J.R., Dillon, M.R., Bokulich, N.A., Abnet, C.C., Al-Ghalith, G.A., Alexander, H., Alm, E.J., Arumugam, M., Asnicar, F., Bai, Y., Bisanz, J.E., Bittinger, K., Brejnrod, A., Brislawn, C.J., Brown, C.T., Callahan, B.J., Caraballo-Rodríguez, A.M., Chase, J., Cope, E.K., Da Silva, R., Diener, C., Dorrestein, P.C., Douglas, G.M., Durall, D.M., Duvallet, C., Edwardson, C.F., Ernst, M., Estaki, M., Fouquier, J., Gauglitz, J.M., Gibbons, S.M., Gibson, D.L., Gonzalez, A., Gorlick, K., Guo, J., Hillmann, B., Holmes, S., Holste, H., Huttenhower, C., Huttley, G.A., Janssen, S., Jarmusch, A.K., Jiang, L., Kaehler, B.D., Kang, K.B., Keefe, C.R., Keim, P., Kelley, S.T., Knights, D., Koester, I., Kosciolek, T., Kreps, J., Langille, M.G.I., Lee, J., Ley, R., Liu, Y.-X., Loftfield, E., Lozupone, C., Maher, M., Marotz, C., Martin, B.D., McDonald, D., McIver, L.J., Melnik, A.V., Metcalf, J.L., Morgan, S.C., Morton, J.T., Naimey, A.T., Navas-Molina, J.A., Nothias, L.F., Orchanian, S.B., Pearson, T., Peoples, S.L., Petras, D., Preuss, M.L., Pruesse, E., Rasmussen, L.B., Rivers, A., Robeson, M.S., Rosenthal, P., Segata, N., Shaffer, M., Shiffer, A., Sinha, R., Song, S.J., Spear, J.R., Swafford, A.D., Thompson, L.R., Torres, P.J., Trinh, P., Tripathi, A., Turnbaugh, P.J., Ul-Hasan, S., van der Hooft, J.J.J., Vargas, F., Vázquez-Baeza, Y., Vogtmann, E., von Hippel, M., Walters, W., Wan, Y., Wang, M., Warren, J., Weber, K. C., Williamson, C.H.D., Willis, A.D., Xu, Z.Z., Zaneveld, J.R., Zhang, Y., Zhu, Q., Knight, R., Caporaso, J.G., 2019. Reproducible, interactive, scalable and extensible microbiome data science using QIIME 2. Nat. Biotechnol. 37 (8), 852–857. https://doi.org/10.1038/s41587-019-0209-9.

Brain, R.A., Hanson, M.L., Solomon, K.R., Brooks, B.W., 2008. Aquatic plants exposed to pharmaceuticals: effects and risks. In: Whitacre, D.M. (Ed.), Rev. Environ. Contam. Toxicol. Springer, New York, New York, NY, pp. 67–115. https://doi.org/10.1007/978-0-387-71724-1_3.

Callahan, B.J., McMurdie, P.J., Rosen, M.J., Han, A.W., Johnson, A.J.A., Holmes, S.P., 2016. DADA2: high-resolution sample inference from Illumina amplicon data. Nat. Methods 13 (7), 581–583. https://doi.org/10.1038/nmeth.3869.

Chopra, I., Hawkey, P.M., Hinton, M., 1992. Tetracyclines, molecular and clinical aspects. J. Antimicrob. Chemother 29 (3), 245–277. https://doi.org/10.1093/jac/29.3.245.

Cid, A., Fidalgo, P., Herrero, C., Abalde, J., 1996. Toxic action of copper on the membrane system of a marine diatom measured by flow cytometry. Cytometry 25 (1), 32–36. https://doi.org/10.1002/(SICI)1097-0320(19960901)25:1<32::AID-CYTO4>3.0.CO;2-G.

Corcoll, N., Yang, J., Backhaus, T., Zhang, X., Eriksson, K.M., 2019. Copper affects composition and functioning of microbial communities in marine biofilms at environmentally relevant concentrations. Front. Microbiol. 9, 3248. https://doi.org/10.3389/fmicb.2018.03248.

Daghrir, R., Drogui, P., 2013. Tetracycline antibiotics in the environment: a review. Environ. Chem. Lett. 11 (3), 209–227. https://doi.org/10.1007/s10311-013-0404-8.

Dawson, S.C., Pace, N.R., 2002. Novel kingdom-level eukaryotic diversity in anoxic environments. Proc. Natl. Acad. Sci. USA 99 (12), 8324–8329. https://doi.org/10.1073/pnas.062169599.

Decelle, J., Romac, S., Sasaki, E., Not, F., Mahé, F., 2014. Intracellular diversity of the V4 and V9 regions of the 18S rRNA in marine protists (radiolarians) assessed by high-throughput sequencing. PLoS One 9 (8), e104297. https://doi.org/10.1371/journal.pone.0104297.

Delaney, S., Jarem, D.A., Volle, C.B., Yennie, C.J., 2012. Chemical and biological consequences of oxidatively damaged guanine in DNA. Free Radic. Res. 46 (4), 420–441. https://doi.org/10.3109/10715762.2011.653968.

Deng, H., He, C., Worden, A.Z., Gong, J., 2024. Employing a triple metabarcoding approach to differentiate active, dormant and dead microeukaryotes in sediments. Environ. Microbiol. 26 (3), e16615. https://doi.org/10.1111/1462-2920.16615.

Díez, B., Pedrós-Alió, C., Marsh Terence, L., Massana, R., 2001. Application of denaturing gradient gel electrophoresis (DGGE) to study the diversity of marine picoeukaryotic assemblages and comparison of DGGE with other molecular techniques. Appl. Environ. Microbiol. 67 (7), 2942–2951. https://doi.org/10.1128/AEM.67.7.2942-2951.2001.

Dover, G., 1982. Molecular drive: a cohesive mode of species evolution. Nature 299 (5879), 111–117. https://doi.org/10.1038/299111a0.

Dykens, J.A., Shick, J.M., 1982. Oxygen production by endosymbiotic algae controls superoxide dismutase activity in their animal host. Nature 297 (5867), 579–580. https://doi.org/10.1038/297579a0.

Falfushynska, H., Lewicka, K., Rychter, P., 2024. Unveiling the hydrochemical and ecotoxicological insights of copper and zinc: impacts, mechanisms, and effective remediation approaches. Limnol. Rev. 24, 406–436. https://doi.org/10.3390/limnolrev24040024.

Festa, R.A., Thiele, D.J., 2011. Copper: an essential metal in biology. Curr. Biol. 21 (21), R877–R883. https://doi.org/10.1016/j.cub.2011.09.040.

Flemming, C.A., Trevors, J.T., 1989. Copper toxicity and chemistry in the environment: a review. Water Air Soil Pollut. 44 (1), 143–158. https://doi.org/10.1007/BF00228784.

Fu, R., Gong, J., 2017. Single cell analysis linking ribosomal (r)DNA and rRNA copy numbers to cell size and growth rate provides insights into molecular protistan ecology. J. Eukaryot. Microbiol. 64 (6), 885–896. https://doi.org/10.1111/jeu.12425.

Gong, J., Dong, J., Liu, X., Massana, R., 2013. Extremely high copy numbers and polymorphisms of the rDNA operon estimated from single cell analysis of Oligotrich and Peritrich ciliates. Protist 164 (3), 369–379. https://doi.org/10.1016/j.protis.2012.11.006.

Gong, J., Qing, Y., Guo, X., Warren, A., 2014. *Candidatus* Sonnebornia yantaiensis", a member of candidate division OD1, as intracellular bacteria of the ciliated protist *Paramecium bursaria* (Ciliophora, Oligohymenophorea). Syst. Appl. Microbiol. 37 (1), 35–41. https://doi.org/10.1016/j.syapm.2013.08.007.

Guillou, L., Bachar, D., Audic, S., Bass, D., Berney, C., Bittner, L., Boutte, C., Burgaud, G., de Vargas, C., Decelle, J., del Campo, J., Dolan, J.R., Dunthorn, M., Edvardsen, B., Holzmann, M., Kooistra, W.H.C.F., Lara, E., Le Bescot, N., Logares, R., Mahé, F., Massana, R., Montresor, M., Morard, R., Not, F., Pawlowski, J., Probert, I., Sauvadet, A.-L., Siano, R., Stoeck, T., Vaulot, D., Zimmermann, P., Christen, R., 2013. The protist ribosomal reference database (PR^2): a catalog of unicellular eukaryote small sub-unit rrna sequences with curated taxonomy. Nucleic Acids Res. 41 (D1), D597–D604. https://doi.org/10.1093/nar/gks1160.

Guo, J., Selby, K., Boxall, A.B.A., 2016. Effects of antibiotics on the growth and physiology of Chlorophytes, Cyanobacteria, and a diatom. Arch. Environ. Contam. Toxicol. 71 (4), 589–602. https://doi.org/10.1007/s00244-016-0305-5.

Hahm, J.Y., Park, J., Jang, E.-S., Chi, S.W., 2022. 8-Oxoguanine: from oxidative damage to epigenetic and epitranscriptional modification. Exp. Mol. Med. 54 (10), 1626–1642. https://doi.org/10.1038/s12276-022-00822-z.

Hamed, S.M., Selim, S., Klöck, G., AbdElgawad, H., 2017. Sensitivity of two green microalgae to copper stress: growth, oxidative and antioxidants analyses. Ecotoxicol. Environ. Saf. 144, 19–25. https://doi.org/10.1016/j.ecoenv.2017.05.048.

He, C., Li, G., Zou, S., Zheng, P., Song, Q., Li, G., Yu, Q., Yu, Y., Zhang, Q., Zhang, X., Shen, Z., Gong, J., 2024. Spatial and diel variations of bacterioplankton and pico-nanoeukaryote communities and potential biotic interactions during macroalgal blooms. Mar. Pollut. Bull. 202, 116409. https://doi.org/10.1016/j.marpolbul.2024.116409.

Hosseini, M.J., Shaki, F., Ghazi-Khansari, M., Pourahmad, J., 2014. Toxicity of copper on isolated liver mitochondria: impairment at complexes I, II, and IV leads to increased ROS production. Cell Biochem. Biophys. 70 (1), 367–381. https://doi.org/10.1007/s12013-014-9922-7.

Hutchings, M.I., Truman, A.W., Wilkinson, B., 2019. Antibiotics: past, present and future. Curr. Opin. Microbiol. 51, 72–80. https://doi.org/10.1016/j.mib.2019.10.008.

Kim, J.S., Kim, H., Yim, B., Rhee, J.S., Won, E.J., Lee, Y.M., 2018. Identification and molecular characterization of two Cu/Zn-SODs and Mn-SOD in the marine ciliate *Euplotes crassus*: modulation of enzyme activity and transcripts in response to copper and cadmium. Aquat. Toxicol. 199, 296–304. https://doi.org/10.1016/j.aquatox.2018.03.020.

Kim, S.H., Jung, M.Y., Lee, Y.M., 2011. Effect of heavy metals on the antioxidant enzymes in the marine ciliate *Euplotes crassus*. Toxicol. Environ. Health Sci. 3 (4), 213–219. https://doi.org/10.1007/s13530-011-0103-4.

Kudryavtsev, A., Gladkikh, A., 2017. Two new species of *Ripella* (Amoebozoa, Vannellida) and unusual intragenomic variability in the SSU rRNA gene of this genus. Eur. J. Protistol. 61, 92–106. https://doi.org/10.1016/j.ejop.2017.09.003.

Laursen, M.F., Dalgaard, M.D., Bahl, M.I., 2017. Genomic GC-content affects the accuracy of 16S rRNA gene sequencing based microbial profiling due to PCR bias. Front. Microbiol. 8, 1934. https://doi.org/10.3389/fmicb.2017.01934.

Li, H., Durbin, R., 2009. Fast and accurate short read alignment with Burrows–Wheeler transform. Bioinformatics 25 (14), 1754–1760. https://doi.org/10.1093/bioinformatics/btp324.

Li, H., Handsaker, B., Wysoker, A., Fennell, T., Ruan, J., Homer, N., Marth, G., Abecasis, G., Durbin, R., Genome Project Data Processing, S., 2009. The sequence alignment/map format and SAMtools. Bioinformatics 25 (16), 2078–2079. https://doi.org/10.1093/bioinformatics/btp352.

Li, X., Gu, A.Z., Zhang, Y., Xie, B., Li, D., Chen, J., 2019. Sub-lethal concentrations of heavy metals induce antibiotic resistance via mutagenesis. J. Hazard. Mater. 369, 9–16. https://doi.org/10.1016/j.jhazmat.2019.02.006.

Liu, Y., Wang, H., Cui, Y., Chen, N., 2023. Removal of copper ions from wastewater: a review. Int. J. Environ. Res. Public Health 20, 3885. https://doi.org/10.3390/ijerph20053885.

Long, H., Miller, S.F., Strauss, C., Zhao, C., Cheng, L., Ye, Z., Griffin, K., Te, R., Lee, H., Chen, C.-C., Lynch, M., 2016. Antibiotic treatment enhances the genome-wide mutation rate of target cells. Proc. Natl. Acad. Sci. USA 113 (18), E2498–E2505. https://doi.org/10.1073/pnas.1601208113.

Martin, M., 2011. Cutadapt removes adapter sequences from high-throughput sequencing reads. EMBnet. J. 17 (1), 10. https://doi.org/10.14806/ej.17.1.200.

Matallana-Surget, S., Meador, J.A., Joux, F., Douki, T., 2008. Effect of the GC content of DNA on the distribution of UVB-induced bipyrimidine photoproducts. Photochem. Photobiol. Sci. 7 (7), 794–801. https://doi.org/10.1039/b719929e.

Morales, M.E., Derbes, R.S., Ade, C.M., Ortego, J.C., Stark, J., Deininger, P.L., Roy-Engel, A.M., 2016. Heavy metal exposure influences double strand break DNA repair outcomes. PLoS. One 11 (3), e0151367. https://doi.org/10.1371/journal.pone.0151367.

Mu, W., Jia, K., Liu, Y., Pan, X., Fan, Y., 2017. Response of the freshwater diatom *Halamphora veneta* (Kützing) Levkov to copper and mercury and its potential for bioassessment of heavy metal toxicity in aquatic habitats. Environ. Sci. Pollut. Res. 24 (34), 26375–26386. https://doi.org/10.1007/s11356-017-0225-6.

Murali, A., Bhargava, A., Wright, E.S., 2018. IDTAXA: a novel approach for accurate taxonomic classification of microbiome sequences. Microbiome 6 (1), 140. https://doi.org/10.1186/s40168-018-0521-5.

Nivedhita, S., Shyni Jasmin, P., Sarvajith, M., Nancharaiah, Y.V., 2022. Effects of oxytetracycline on aerobic granular sludge process: granulation, biological nutrient removal and microbial community structure. Chemosphere 307, 136103. https://doi.org/10.1016/j.chemosphere.2022.136103.

Pawlowski, J., Audic, S., Adl, S., Bass, D., Belbahri, L., Berney, C., Bowser, S.S., Cepicka, I., Decelle, J., Dunthorn, M., Fiore-Donno, A.M., Gile, G.H., Holzmann, M., Jahn, R., Jirků, M., Keeling, P.J., Martin Kostka, A.K., Lara, E., Lukeš, J., David G Mann, E.AD., Mitchell, F., Nitsche, M., Romeralo, G.W, Saunders, A., Simpson, G.B, Smirnov, A.V, Spouge, J.L, Stern, R.F, Stoeck, T., Zimmermann, J., Schindel, D., de Vargas, C., 2012. CBOL protist working group: barcoding eukaryotic richness beyond the animal, plant, and fungal kingdoms. PLoS Biol. 10 (11), e1001419. https://doi.org/10.1371/journal.pbio.1001419.

Poetsch, A.R., 2020. The genomics of oxidative DNA damage, repair, and resulting mutagenesis. Comput. Struct. Biotechnol. J. 18, 207–219. https://doi.org/10.1016/j.csbj.2019.12.013.

Prezant, T.R., Agapian, J.V., Bohlman, M.C., Bu, X., Öztas, S., Qiu, W.-Q., Arnos, K.S., Cortopassi, G.A., Jaber, L., Rotter, J.I., Shohat, M., Fischel-Ghodsian, N., 1993. Mitochondrial ribosomal RNA mutation associated with both antibiotic–induced and non-syndromic deafness. Nat. Genet. 4 (3), 289–294. https://doi.org/10.1038/ng0793-289.

Qin, Y., Wu, L., Zhang, Q., Wen, C., Van Nostrand Joy, D., Ning, D., Raskin, L., Pinto, A., Zhou, J., 2023. Effects of error, chimera, bias, and GC content on the accuracy of amplicon sequencing. mSystems 8 (6), e01025. https://doi.org/10.1128/msystems.01025-23. -01023.

Reichenberger, E.R., Rosen, G., Hershberg, U., Hershberg, R., 2015. Prokaryotic nucleotide composition is shaped by both phylogeny and the environment. Genome Biol. Evol. 7 (5), 1380–1389. https://doi.org/10.1093/gbe/evv063.

Revitt-Mills, S.A., Robinson, A., 2020. Antibiotic-induced mutagenesis: under the microscope. Front. Microbiol. 11, 585175. https://doi.org/10.3389/fmicb.2020.585175.

Seixas, A.F., Quendera, A.P., Sousa, J.P., Silva, A.F.Q., Arraiano, C.M., Andrade, J.M., 2022. Bacterial response to oxidative stress and RNA oxidation. Front. Genet. 12, 821535. https://doi.org/10.3389/fgene.2021.821535.

Shakya, M., Silvester, E., Rees, G., Rajapaksha, K.H., Faou, P., Holland, A., 2022. Changes to the amino acid profile and proteome of the tropical freshwater microalga *Chlorella* sp. in response to copper stress. Ecotoxicol. Environ. Saf. 233, 113336. https://doi.org/10.1016/j.ecoenv.2022.113336.

Shcherbik, N., Pestov, D.G., 2019. The impact of oxidative stress on ribosomes: from injury to regulation. Cells 8 (11), 1379. https://doi.org/10.3390/cells8111379.

Siedlewicz, G., Żak, A., Sharma, L., Kosakowska, A., Pazdro, K., 2020. Effects of oxytetracycline on growth and chlorophyll a fluorescence in green algae (*Chlorella vulgaris*), diatom (*Phaeodactylum tricornutum*) and cyanobacteria (*Microcystis aeruginosa* and *Nodularia spumigena*). Oceanologia 62 (2), 214–225. https://doi.org/10.1016/j.oceano.2019.12.002.

Sigmund, C.D., Ettayebi, M., Morgan, E.A., 1984. Antibiotic resistance mutations in 16S and 23S ribosomal RNA genes of *Escherichia coli*. Nucleic Acids Res. 12 (11), 4653–4664. https://doi.org/10.1093/nar/12.11.4653.

Simms, C.L., Zaher, H.S., 2016. Quality control of chemically damaged RNA. Cell Mol. Life Sci. 73 (19), 3639–3653. https://doi.org/10.1007/s00018-016-2261-7.

Slaveykova, V., Sonntag, B., Gutiérrez, J.C., 2016. Stress and protists: no life without stress. Eur. J. Protistol. 55, 39–49. https://doi.org/10.1016/j.ejop.2016.06.001.

Somasundaram, S., Abraham, J.S., Maurya, S., Makhija, S., Gupta, R., Toteja, R., 2018. Cellular and molecular basis of heavy metal-induced stress in ciliates. Curr. Sci. 114 (9), 1858. https://doi.org/10.18520/cs/v114/i09/1858-1865.

Somasundaram, S., Abraham, J.S., Maurya, S., Toteja, R., Gupta, R., Makhija, S., 2019. Expression and molecular characterization of stress-responsive genes (hsp70 and Mn-sod) and evaluation of antioxidant enzymes (CAT and GPx) in heavy metal exposed freshwater ciliate. *Tetmemena* sp. Mol. Biol. Rep. 46 (5), 4921–4931. https://doi.org/10.1007/s11033-019-04942-0.

Summerer, M., Sonntag, B., Hörtnagl, P., Sommaruga, R., 2009. Symbiotic ciliates receive protection against UV damage from their algae: a test with *Paramecium bursaria* and *Chlorella*. Protist 160 (2), 233–243. https://doi.org/10.1016/j.protis.2008.11.005.

Thornton, K., Kwan, E.X., Bubb, K., Paleologu, L., Raghuraman, M.K., Brewer, B.J., Cuperus, J.T., Queitsch, C., 2024. rDNA copy number variation in yeast alters response to environmental conditions. bioRxiv (30), 615902. https://doi.org/10.1101/2024.09.30.615902.

Tsvetkov, P., Coy, S., Petrova, B., Dreishpoon, M., Verma, A., Abdusamad, M., Rossen, J., Joesch-Cohen, L., Humeidi, R., Spangler, R.D., Eaton, J.K., Frenkel, E., Kocak, M., Corsello, S.M., Lutsenko, S., Kanarek, N., Santagata, S., Golub, T.R., 2022. Copper induces cell death by targeting lipoylated TCA cycle proteins. Science (1979) 375 (6586), 1254–1261. https://doi.org/10.1126/science.abf0529.

Wang, C., Pan, X., Fan, Y., Chen, Y., Mu, W., 2017. The oxidative stress response of oxytetracycline in the ciliate *Pseudocohnilembus persalinus*. Environ. Toxicol. Pharmacol. 56, 35–42. https://doi.org/10.1016/j.etap.2017.08.019.

Wang, L., Chen, Y., Zhao, Y., Du, M., Wang, Y., Fan, J., Ren, N., Lee, D.-J., 2020. Toxicity of two tetracycline antibiotics on *Stentor coeruleus* and *Stylonychia lemnae*: potential use as toxicity indicator. Chemosphere 255, 127011. https://doi.org/10.1016/j.chemosphere.2020.127011.

Wang, Y., Gong, X., Huang, D., Zhang, J., 2022. Increasing oxytetracycline and enrofloxacin concentrations on the algal growth and sewage purification performance of an algal-bacterial consortia system. Chemosphere 286, 131917. https://doi.org/10.1016/j.chemosphere.2021.131917.

Wang, Y., Meng, T., Zhang, L., Lin, Y., Wu, N., Yuan, H., He, Z., Niu, Y., Dai, Y., Zhao, X., Duan, H., 2023. Inhalable mixture of polycyclic aromatic hydrocarbons and metals, DNA oxidative stress and nasal ribosomal DNA copy number amplification: direct and indirect effect analyses among population. J. Hazard. Mater. 455, 131538. https://doi.org/10.1016/j.jhazmat.2023.131538.

Weber, A.A.T., Pawlowski, J., 2013. Can abundance of protists be inferred from sequence data: a case study of Foraminifera. PLoS One 8 (2), e56739. https://doi.org/10.1371/journal.pone.0056739.

Weber, A.A.T., Pawlowski, J., 2014. Wide occurrence of SSU rDNA intragenomic polymorphism in foraminifera and its implications for molecular species identification. Protist 165 (5), 645–661. https://doi.org/10.1016/j.protis.2014.07.006.

Weider, L.J., Elser, J.J., Crease, T.J., Mateos, M., Cotner, J.B., Markow, T.A., 2005. The functional significance of ribosomal (r)DNA variation: impacts on the evolutionary ecology of organisms. Annu Rev. Ecol. Evol. Syst. 36, 219–242. https://doi.org/10.1146/annurev.ecolsys.36.102003.152620, 362005.

Weissman, J.L., Fagan, W.F., Johnson, P.L.F., 2019. Linking high GC content to the repair of double strand breaks in prokaryotic genomes. PLoS Genet. 15 (11), e1008493. https://doi.org/10.1371/journal.pgen.1008493.

Willi, J., Küpfer, P., Evéquoz, D., Fernandez, G., Katz, A., Leumann, C., Polacek, N., 2018. Oxidative stress damages rRNA inside the ribosome and differentially affects the catalytic center. Nucleic Acids Res. 46 (4), 1945–1957. https://doi.org/10.1093/nar/gkx1308.

Yu, Y., Li, G., Zhang, H., Hu, Z., Yu, D., Gong, J., 2025. Seasonally and niche-differentiated diversity of active, dormant and dead microbes in coastal waters and surface sediments. Commun. Biol. 8 (1), 1388. https://doi.org/10.1038/s42003-025-08789-z.

Zhang, Y., Wen, Y., Xiao, Q., Zheng, W., Long, G., Chen, B., Shu, X., Jiang, M., 2020. Mutations in the antibiotic target genes related to clarithromycin, metronidazole and levofloxacin resistance in *Helicobacter pylori* strains from children in China. Infect. Drug Resist. Volume 13 (null), 311–322. https://doi.org/10.2147/IDR.S235615.

Zhong, X., Zhu, Y., Wang, Y., Zhao, Q., Huang, H., 2021. Effects of three antibiotics on growth and antioxidant response of *Chlorella pyrenoidosa* and *Anabaena cylindrica*. Ecotoxicol. Environ. Saf. 211, 111954. https://doi.org/10.1016/j.ecoenv.2021.111954.

Zou, S., Zhang, Q., Zhang, X., Dupuy, C., Gong, J., 2020. Environmental factors and pollution stresses select bacterial populations in association with protists. Front. Mar. Sci. 7, 659. https://doi.org/10.3389/fmars.2020.00659.

Zou, S., Fu, R., Deng, H., Zhang, Q., Gentekaki, E., Gong, J., 2021. Coupling between ribotypic and phenotypic traits of protists across life cycle stages and temperatures. Microbiol. Spectr. 9 (3), e01738. https://doi.org/10.1128/Spectrum.01738-21.-01721.

Zou, S., Lian, Q., Ni, M., Zhou, D., Liu, M., Zhang, X., Chen, G., Yuan, J., 2024. Spatiotemporal assembly and functional composition of planktonic microeukaryotic communities along productivity gradients in a subtropical lake. Front. Microbiol. 15, 1351772. https://doi.org/10.3389/fmicb.2024.1351772.